SUPPORTING INFORMATION

Digital diffraction analysis enables low-cost molecular diagnostics on a smartphone

Hyungsoon Im[a,b,1], Cesar M. Castro[a,c,1], Huilin Shao[a], Monty Liong[a,2], Jun Song[a,d], Divya Pathania[a,b], Lioubov Fexon[a], Changwook Min[a], Maria Avila-Wallace[e], Omar Zurkiya[a,b], Junsung Rho[a], Brady Magaoay[a], Rosemary H. Tambouret[f], Misha Pivovarov[a,b], Ralph Weissleder[a,b,g,3], Hakho Lee[a,b,3].

[a] Center for Systems Biology, Massachusetts General Hospital, 185 Cambridge St, CPZN 5206, Boston, MA 02114.

[b] Department of Radiology, Massachusetts General Hospital, Boston, MA 02114.

[c] Massachusetts General Hospital Cancer Center, Harvard Medical School, 55 Fruit St - Yawkey 9E, Boston, MA 02114.

[d] School of Engineering and Applied Sciences, Harvard University, Cambridge, MA 02138.

[e] Department of Obstetrics and Gynecology, Massachusetts General Hospital, Boston, MA 02114.

[f] Department of Pathology, Massachusetts General Hospital, Boston, MA 02114.

[g] Department of Systems Biology, Harvard Medical School, 200 Longwood Ave, Boston, MA 02115.

[1]H.I. and C.M.C. contributed equally to this work.
[2]Present address: Cardno ChemRisk, San Francisco, CA 94105.

[3]To whom correspondence may be addressed. Email: rweissleder@mgh.harvard.edu or hlee@mgh.harvard.edu.

Supplementary Materials and Methods

Cell preparation

SkBr3 and A431 human cancer cells were cultured in DMEM medium and supplemented with fetal bovine serum (10%), penicillin and streptomycin (1%) and L-glutamine (1%). Cell lines were maintained at 37°C in a humidified atmosphere containing 5% CO_2 and used when at confluence. Cells were washed, trypsinized and resuspended in a binding buffer (1× phosphate buffer saline/ PBS containing 2% fetal bovine serum and 1% BSA; PBS+). In a typical labeling experiment, 10^5 cells were labeled in two steps: biotinylated anti-HER2, anti-EpCAM or anti-EGFR (2 μg/mL, 8 biotin molecules/antibody) and streptavidin-coated polystyrene particles (0.5 mg, 7 μm diameter, Spherotech), each for 10 min at room temperature. Following this procedure, the averaged number of beads non-specifically bound to cells was maintained at < 0.2 beads per cell. Leukocytes were prepared from 0.6 ml blood samples mixed with 12 mL BD Phosflow Lyse/Fix buffer (1×) for 15 min at 37 °C. The cells were resuspended in PBS+ and serially diluted for quantitative analyses on counting.

Fluorescence measurements

SkBr3 and A431 human cancer cells were labeled with fluorescent antibodies (2 μg/mL) for 20 min at room temperature. Following aspiration and centrifugation, the cells were fixed for measurements using BD Fix Buffer (BD Biosciences). Flow cytometry measurements used BD LSR II flow cytometer, and mean fluorescence intensity was determined using FlowJo software. For labeling live cells and microscopy imaging, cells were grown to confluency in an 8-well chamber slide. After being washed with PBS+, the cells were labeled as described above, except that cell culture medium was used instead of PBS+. The cells were then fixed and permeabilized with BD Fix Buffer and BD Perm/Wash Buffer for 20 min before incubating in a solution of TO-PRO-1 iodide (1 μM in BD Perm/Wash Buffer) for 15 min.
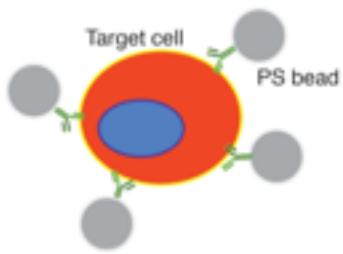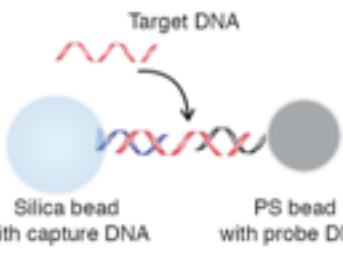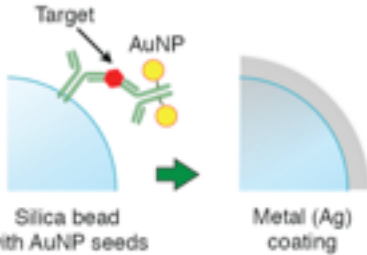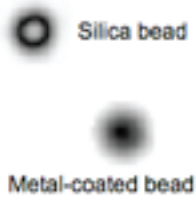
HPV DNA detection

The bead-based DNA assay was designed using a similar method previously described by our group(1). Target sequences (~50 nucleotides) unique to HPV 16 and HPV 18 DNA were selected for hybridization based sandwich assay. Pairs of specific oligonucleotide probes (~22 nucleotides) were designed to be complementary to sequences within the target regions of HPV 16 and HPV 18 DNA, with one hybridizing to a 5′ end of the target and the other to the 3′ end. One of the probes had a thiol modification at 5' end for attaching it onto the amine modified 6 μm polystyrene beads (Polysciences Inc.), and the other had 3' biotin modification to react with avidin activated 7 μm silica beads (Corpuscular Inc). Several adenine residues (Poly A) were added to the outer end of the probes, with the functional group (thiol or biotin) at the terminal end of the polyA linker. All oligonucleotides were custom-synthesized by Integrated DNA Technologies. In the presence of target HPV DNA, the polystyrene-silica bead dimerized and generated exhibited unique diffraction signature. The bead dimers were then counted using the D3 platform to quantify the amount of target DNA. HPV DNA sequences for HPV 16 is "TGG TGG GTG TAG CTT TTC GTT TTC CTA ATG TAA ATT TTG GTT TGG CCT TCA ATC CTG C"

and the sequences for HPV 18 is "GTA TGG TAT CCC ACC GTG CCG CAC GAC GCA AAC GGG CTT CGG TAA CTG ACT T"

Clinical lymph node samples

FNA samples were mixed collagenase (0.2 mg/mL, Sigma-Aldrich) to breakdown any clumps present in the sample. Cells were then fixed using 1× BD Phosflow Lyse/Fix buffer (BD Biosciences), washed (300 × g) with PBS (2% BSA), and then blocked in FcR blocking solution (4 parts PBS with 0.5% BSA and 1 part FcR blocking reagent, human, Miltenyi Biotech) at room temperature (RT). Subsequently, samples were labeled with primary antibodies for 15 min at RT. After being washed with FcR blocking solution, samples were incubated with microbeads coated with goat anti-mouse IgG secondary antibody (Invitrogen) for 20 min at RT.

Table S1. D3 assay configurations for different detection targets. For cells, immunomicrobeads in different sizes and optical transmittance bind to specific markers on extracellular membranes. For nucleic acids, two different types of microbeads, coated with oligonucleotides complementary to each side of target DNA, dimerize. For proteins, a sandwich assay with affinity ligands (e.g. peptide, antibodies) is used to coat the silica microbead surface with Au nanoparticles, subsequently converted to a metallic film. The changes in light transmittance of metal-coated silica beads are detected by the D3 platform.

Targets	Assay type	Optical signature
Cell	Target cell, PS bead	Beads bound to cells
Nucleic acid	Target DNA; Silica bead with capture DNA, PS bead with probe DNA	Formation of PS-silica dimers
Protein	Target, AuNP; Silica bead with AuNP seeds, Metal (Ag) coating	Silica bead, Metal-coated bead — Changes in transmittance

PS, polystyrene

Table S2. Comparison of hardware setup and computational time in different diffraction-based system. Unknown information is left in blank.

	D3 server	MacBook pro	Ref S1	Ref S2	Ref S3
Model	HP xw4600	MD322LL/A			
CPU	3.16 GHz Core2 Duo E8500	2.4 GHz Core i5	3.2 GHz PC	Intel i7	1.8 GHz Dual Core
Memory	8GB	8GB			
GPU	Tesla C-2070	AMD Radeon HD 6770M (Not used)	Used		-
Language	C++	Matlab	Matlab		Matlab
Cost	$4,051 in 2011	$2,199 in 2012			
Calculation time	0.09 sec (1024x1024 image)	264 sec (1024x1024 image)	0.2 sec	2 - 3 min	10 min
Function	Image reconstruction and molecular quantification	Image reconstruction and molecular quantification	Reconstruction	Reconstruction in sub-pixel resolution	Deconvolution of a fluorescence image

S1. Bishara et al., 2010, Opt Exp, 18, 27499-510
S2. Zheng et al., 2011, Proc Natl Acad Sci U S A, 108, 16889-94
S3. Coskun et al., 2010, Lab Chip, 10, 824-7

Table S3. D3 assay and image analysis time. Once cells are harvested, immunolabeling can be completed within 40 min and imaging acquisition, analysis and final readout can be done in 5 min.

Procedure		Time	Data size
Antibody incubation		10 - 30 min	
Bead incubation		< 10 min	
Image acquisition		< 10 sec	24 mega bytes (MB)
Data transfer / analysis	Data transfer	< 1 min (Wi-Fi) 2 - 3 min (2G)	2.9 MB (zip)
	Data analysis in the GPU server	< 1 sec	
	Test result transfer	< 1 min	1 kilo byte text 1 MB image
Read final result and images		< 1 min	
Total		< 45 min	< 4 MB (transfer)

Table S4. D3 hardware and single assay cost for cellular detention and profiling. The cost is based on today's end-user catalog prices from commercial vendors.

	Name	Current cost*	Current cost per single assay*
Antibodies	EpCAM	$339 (500 µg)	$0.17
	CD44	$118 (500 µg)	$0.06
	Trop2	$323 (100 µg)	$0.80
Beads	Streptavidin-coated polystyrene microbeads	$225 (0.5% w/v, 5 mL)	$0.45
Others	misc reagents (e.g. buffer solutions, tubes)		$0.34
Hardware	iPhone 4S	$145.00	-
	Snap-on module	$6 (LED, switch, battery) $5 (Plastic mount) $20 (pin hole) $25 (lens)	-

Total hardware cost: $200; single assay cost: $1.8

*The current cost figures are based on commercial products for end-users and would decrease with bulk orders upon scale up.
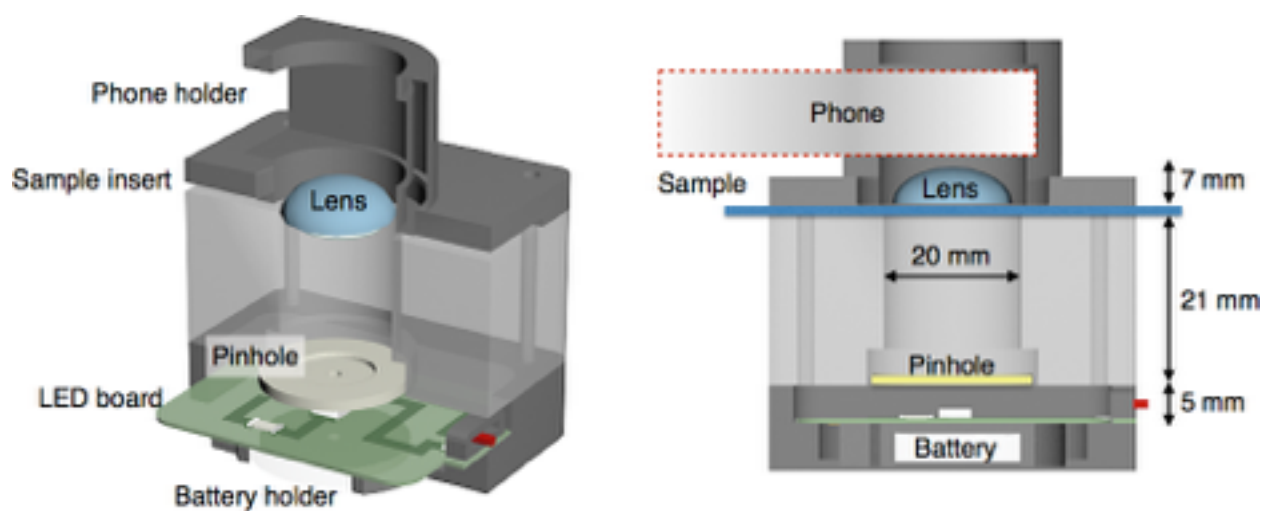
Fig. S1. Cross-section geometry of the smartphone snap-on module. Figures are not drawn to scale.
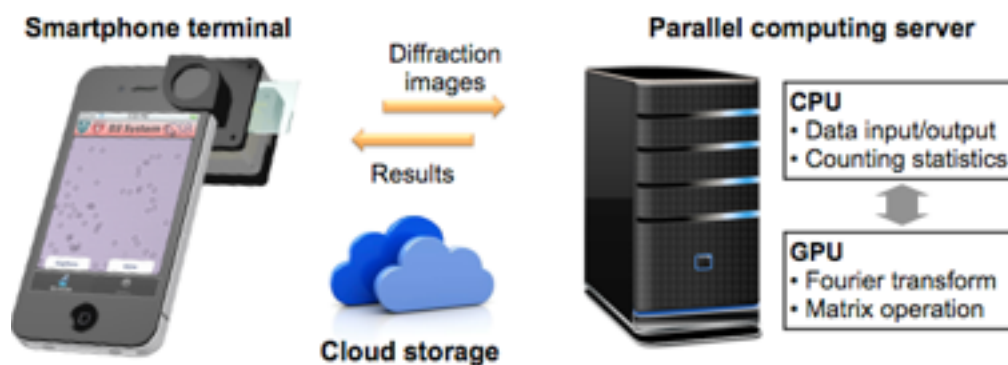
Fig. S2. Digital diffraction diagnostic (D3) technology. Diffraction patterns imaged by a smartphone terminal are transferred to cloud storage over wireless network. Upon downloading a new data, the host server reconstructs the original object images and analyzes them (e.g., cell and bead counting). The server-processes are expedited via a parallel computing with a graphical processing unit (GPU). The reconstructed images and analysis results are then posted to the cloud storage for readout from the smartphone.
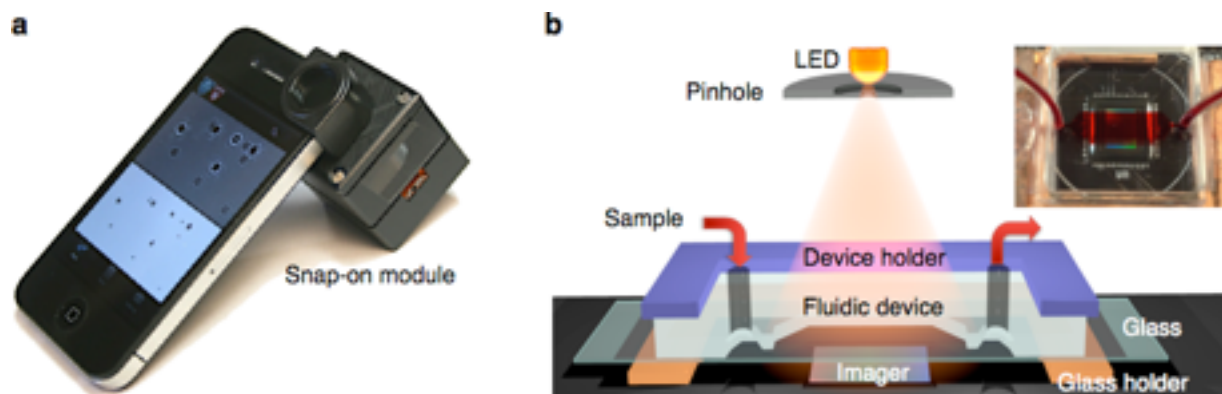
Fig. S3. Implemented digital diffraction diagnostic (D3) platforms. (a) Smartphone-based system. iPhone 4s (Apple) was adopted as the imaging terminal. The snap-on module was attached in front of the embedded camera. The module housed a lighting source, and provided a guide for sample insert. **(b)** Imager IC (integrated circuit)-based system. The device combined the D3 with microfluidics to provide high throughput, in-flow measurements. The fluidic device was bonded to a glass coverslip (thickness, 160 μm), and placed right above the imager. (Inset) Samples were delivered to the imaging area through a microfluidic channel.
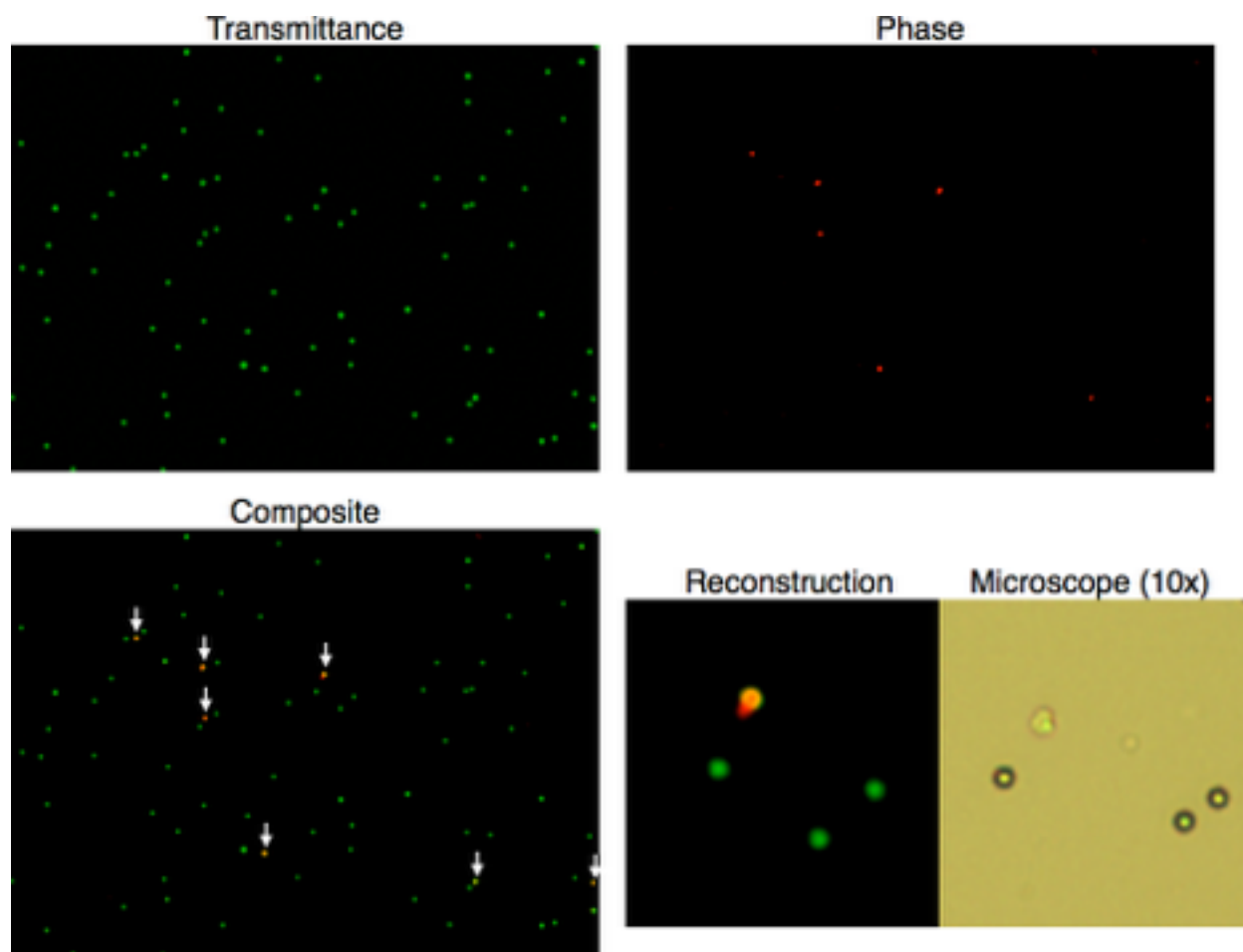
**Fig. S4. Reconstructed transmittance and phase images of white blood cells (WBCs) and 7 μm polystyrene bead mixtures.** Due to their similar size, cells and beads are difficult to distinguish in transmittance images. The addition of phase images, however clearly separates the two and identifies WBCs (indicated by arrows).
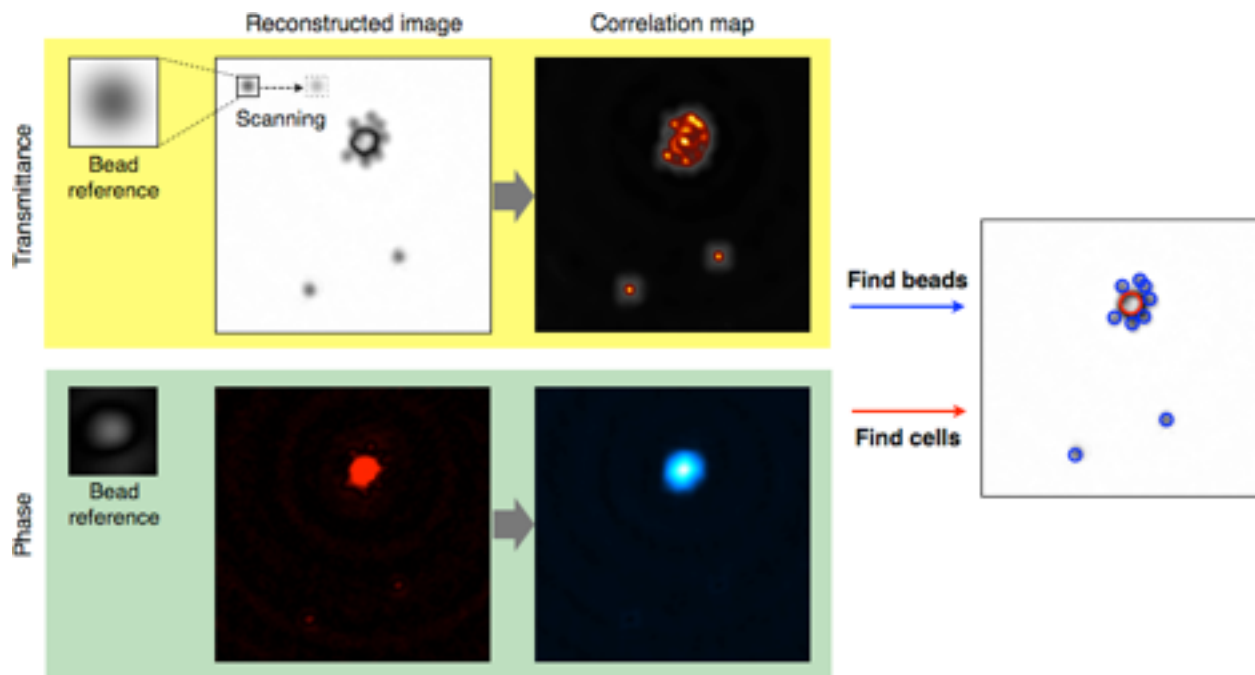
Fig. S5. Principle of counting algorithm. Cells and beads are detected based on transmittance and phase correlation maps. The transmittance correlation map is generated by scanning the transmittance of a reference bead over that of a reconstructed image (top). The phase correlation map is generated in a similar manner using phase information (bottom). The beads are identified in the transmittance correlation map, whereas the cells are detected in the phase correlation map.
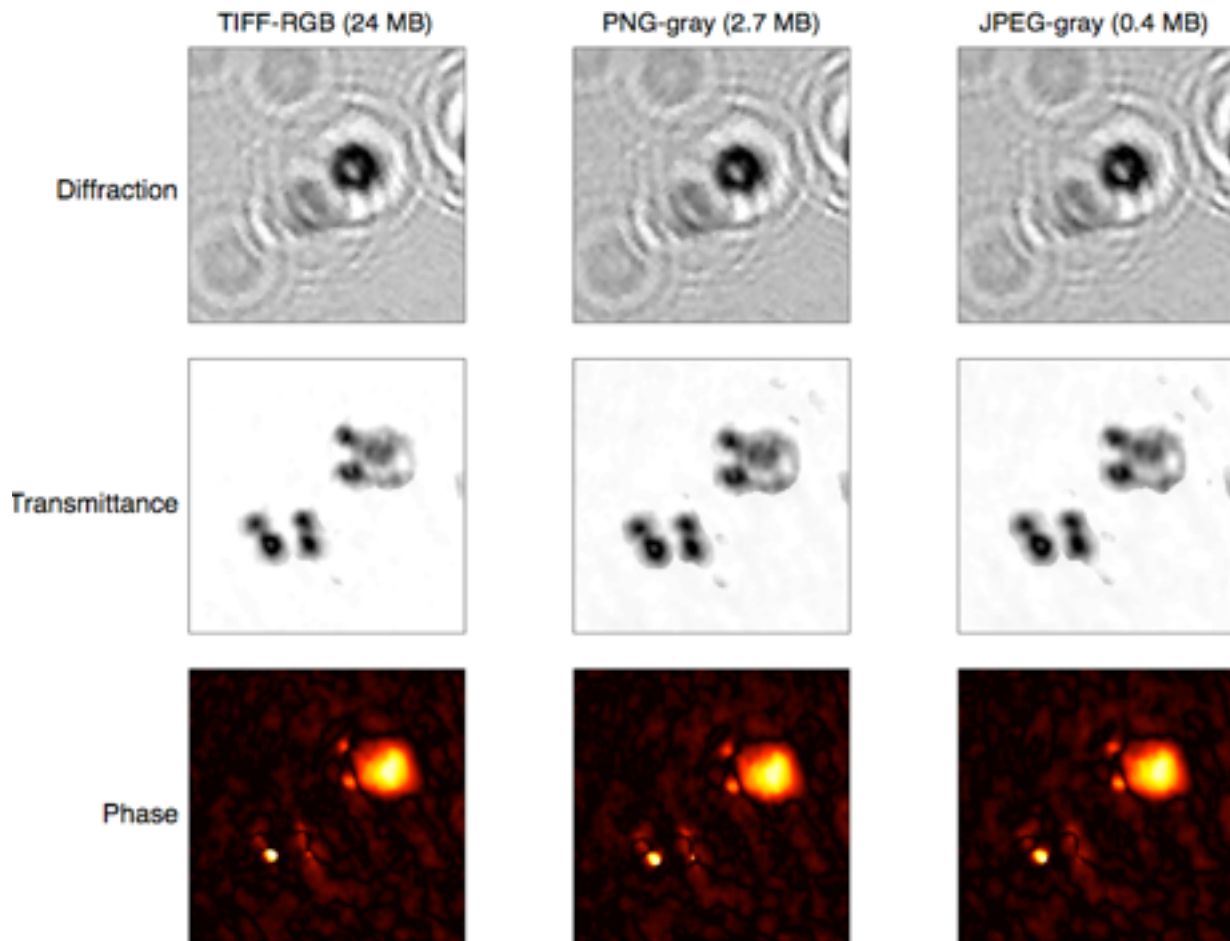
Fig. S6. Image compression for faster file transfer. The original diffraction images (top row) from a smartphone are compressed into a loss-less gray-scale PNG format, which reduces the file size by 89%. When the object size is > 5 μm, the images can be further converted to a JPEG format (right) without compromising the bead and the cell count results. The final file size is 1.6% of its original value, and can be transferred to a cloud server in less than 3 minutes even via slow cellular network (2G).
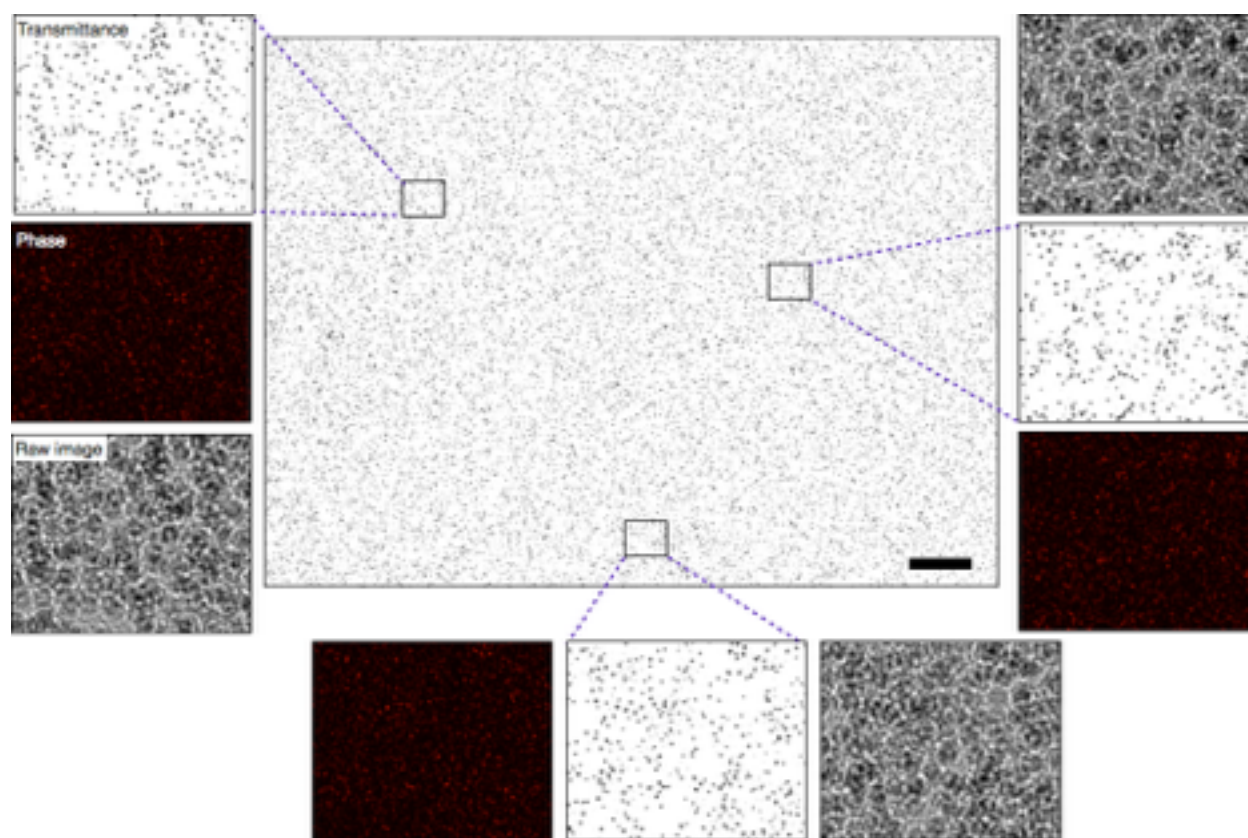
Fig. S7. Reconstructed images of microbeads. Polystyrene microbeads (diameter, 7 μm) were imaged at a high concentration ($\sim$4 × 10^8 beads/mL) using a field-of-view of 24 mm^2. About 150,000 beads were imaged and detected from a single image. Reconstructed amplitude, phase and raw diffraction images are shown for three selected spots. Note that microbeads are highly visible only in transmittance images. Scale bar, 500 μm.
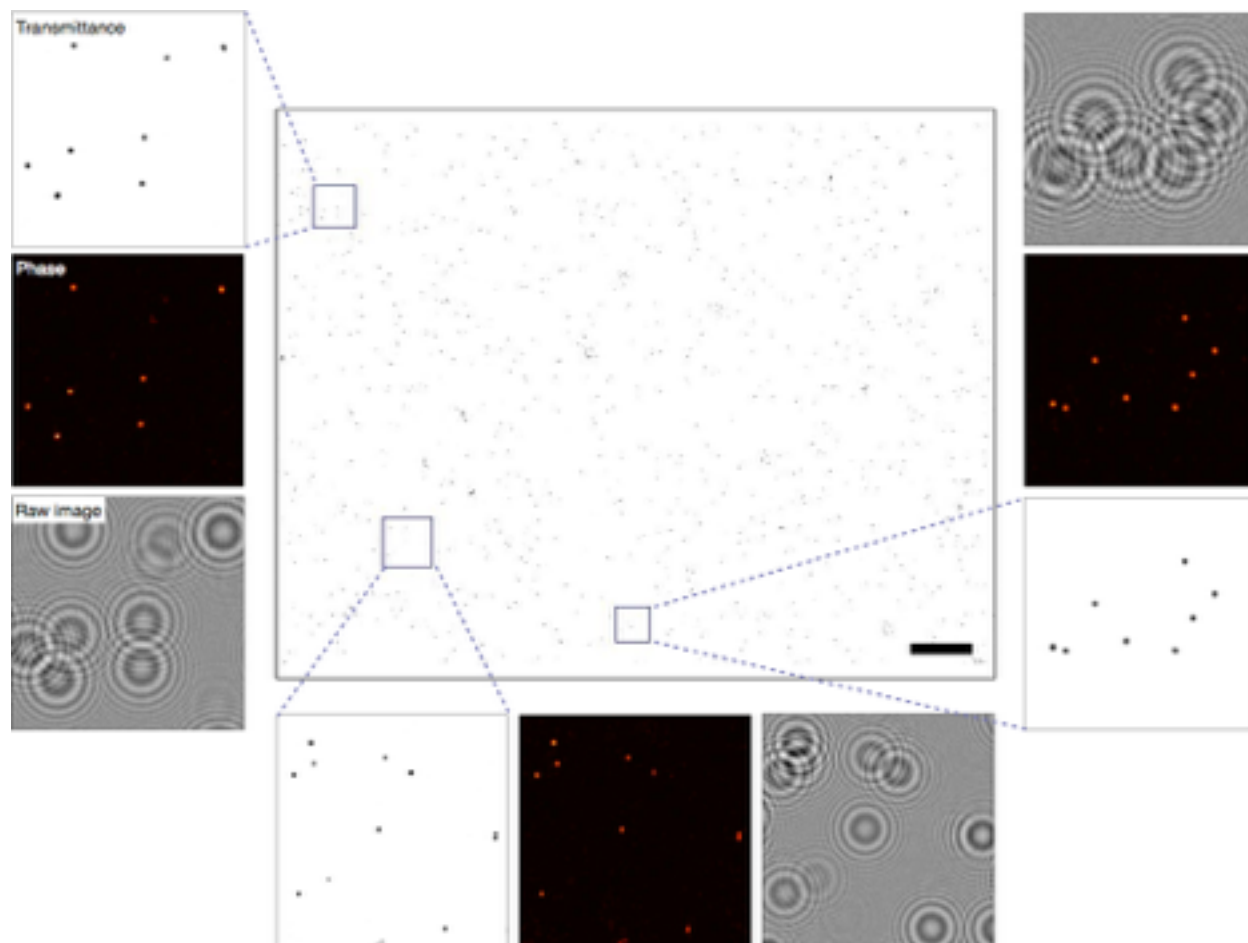
Fig. S8. Reconstructed images of leukocytes. Human leukocytes at a physiological concentration (~5 × 10^6 cells/mL) were imaged using a field-of-view of 24 mm^2. About 1,300 leukocytes were imaged and detected from this single image. Reconstructed amplitude, phase and raw diffraction images are shown for three selected spots. Unlike polystyrene microbeads, leukocytes are highly visible both in transmittance and phase images. Scale bar, 500 μm.
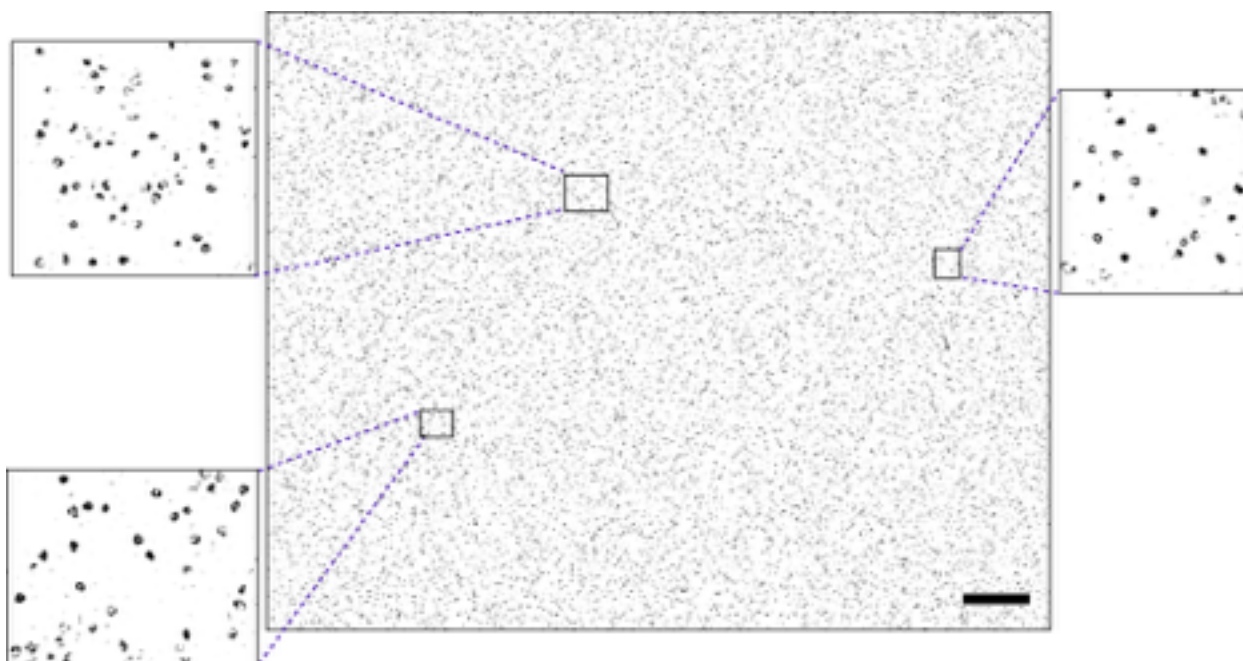
Fig. S9. Reconstructed images of lymphoma cells. Human lymphoma cells (Daudi) at a high concentration (~10^8 cells/mL) were imaged using a field-of-view of 24 mm². About 50,000 Daudi were imaged and detected from this single image. Reconstructed amplitude images are shown for three selected spots. Scale bar, 500 μm.
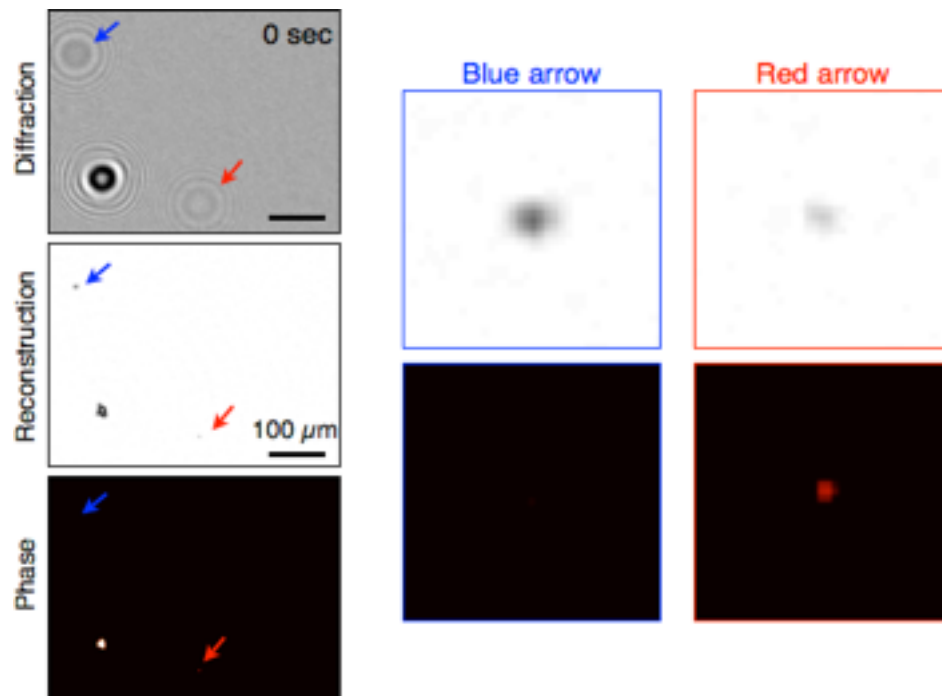
Fig. 10. Differentiation of bead and non-targeted cells. Phase contrast image of objects shown in Fig. 3C (main text) can differentiate a non-targeted cell (red) from a free-floating microbead (blue).
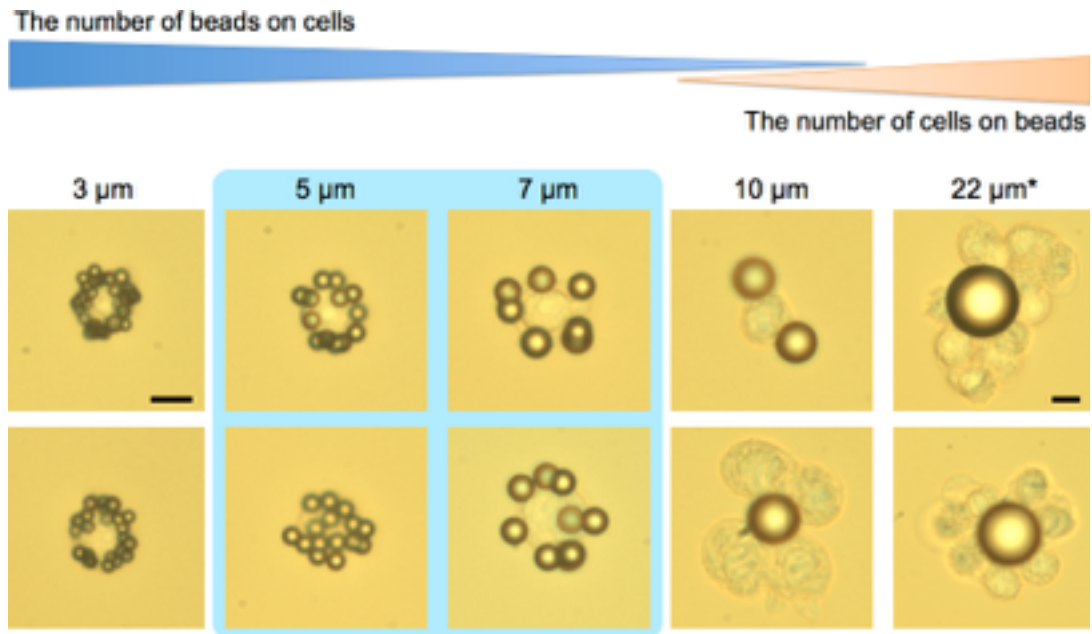
Fig. S11. Optimization of microbead size for cell labeling. Microscope images of cancer cells labeled with differently sized microbeads. The number of beads bound to cells decreased with the bead diameter up to 10 μm. When the diameter was >10 μm, multiple cells were aggregated around a single microbead. The micrographs for 22-μm beads are down-scaled by 70%. Scale bar, 10 μm.
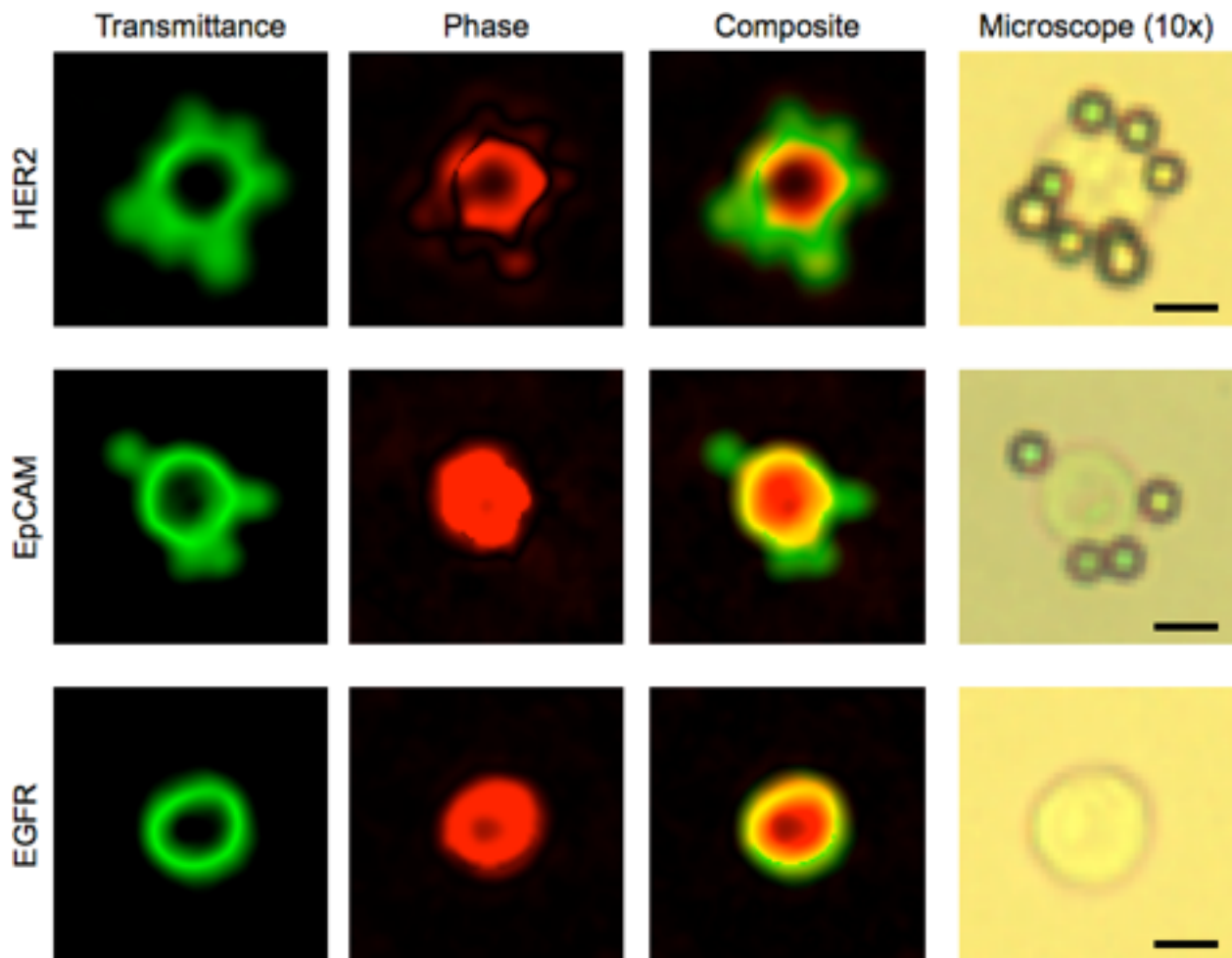
Fig. S12. Recognition of cells and microbeads. While both cells and beads were visible in reconstructed transmittance images (green channel), only cells were highly visible in phase images (red channel). Thereby, cells and beads were distinguishable in composite images by the developed detection algorithm. The expression levels of target markers were determined by counting the number of immunobeads attached to cells. The transmittance (green) and phase contrast (red) images are pseudo-colored to better visualize optical properties of cells and beads. Scale bar, 10 μm.
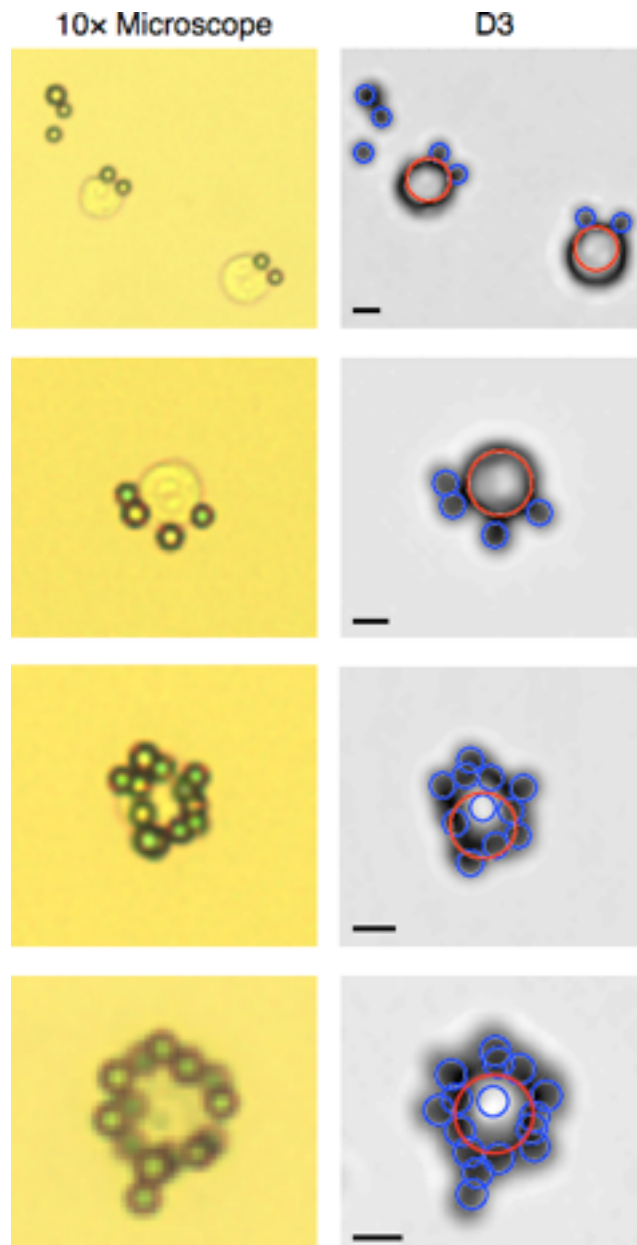
Fig. S13. Cancer cells labeled with different numbers of microbeads. Reconstructed images (right) are compared with conventional bright-field micrographs (left). Both cancer cells and 7-μm microbeads are accurately detected by the detection algorithm. Scale bar, 10 μm.
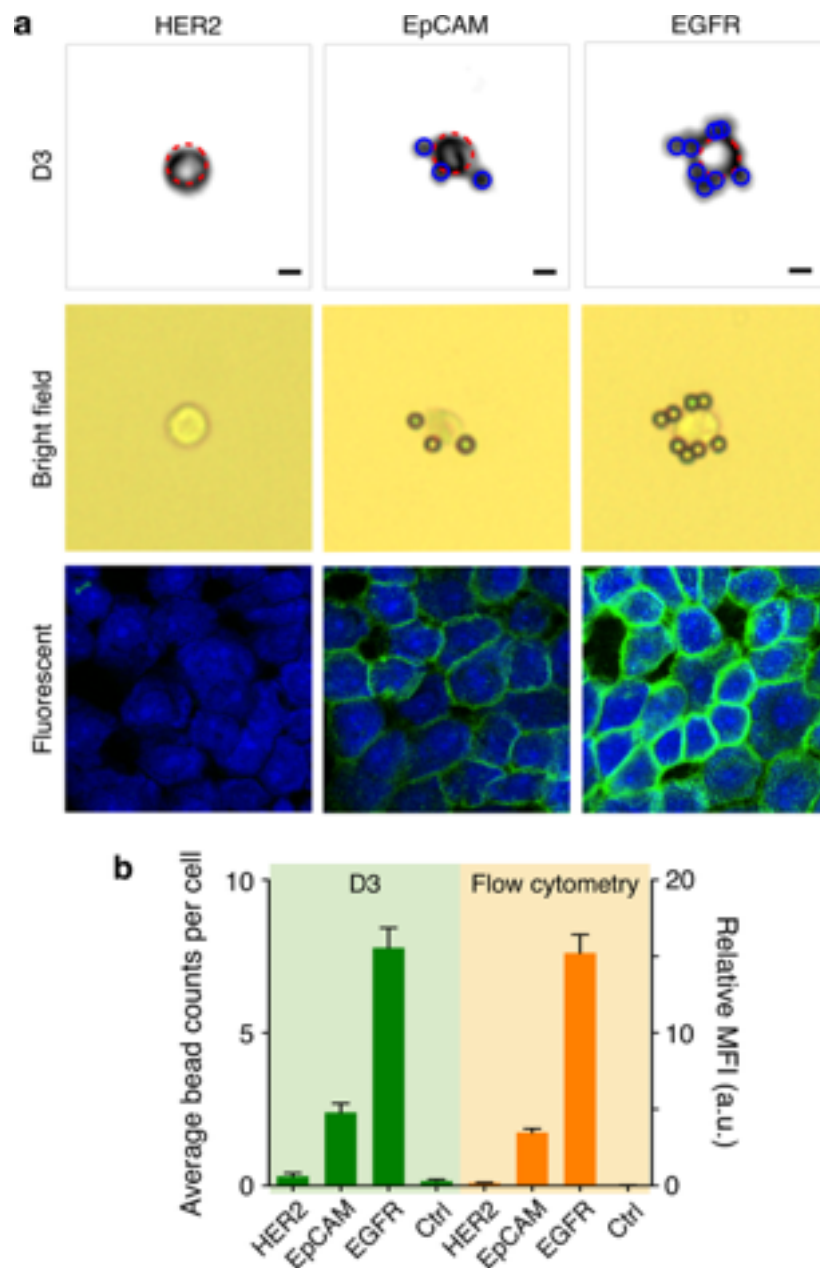
Fig. S14. Molecular profiling of A431 cancer cells. (a) Reconstructed images of A431cells labeled for HER2, EpCAM, and EGFR immunobeads (7 μm, top row) are compared with corresponding bright-field microscope images (middle row). The number of beads on the cells correlates with the expression level of a target marker (bottom row). **(b)** The average number of beads per cell showed an excellent match with the mean fluorescence intensity (MFI) from flow cytometry (R^2 = 0.99). Scale bar, 10 μm.
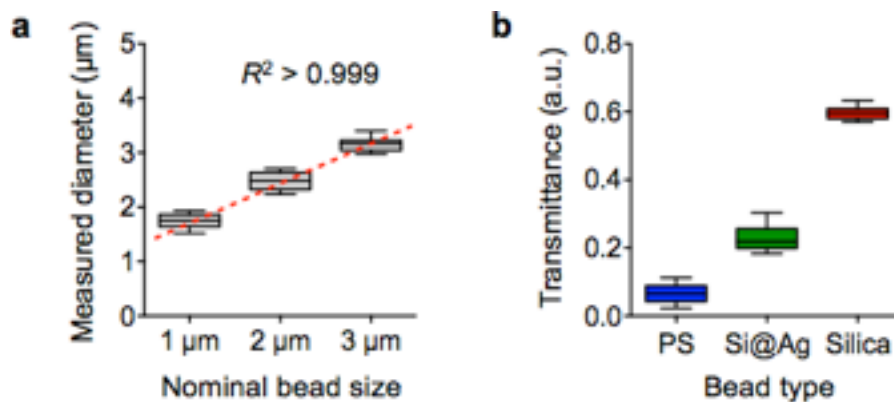
Fig. S15. Multiplexing with different sizes and transmittance of beads. (a) Three different sizes of beads (1, 2 and 3 *μ*m) were imaged using the D3 platform. The measured bead diameters were matched with nominal values. **(b)** The transmittance measured by the D3 platform was different depending on optical properties of bead materials. PS, polystyrene microbeads; Si@Ag, silica microbeads coated with silver.
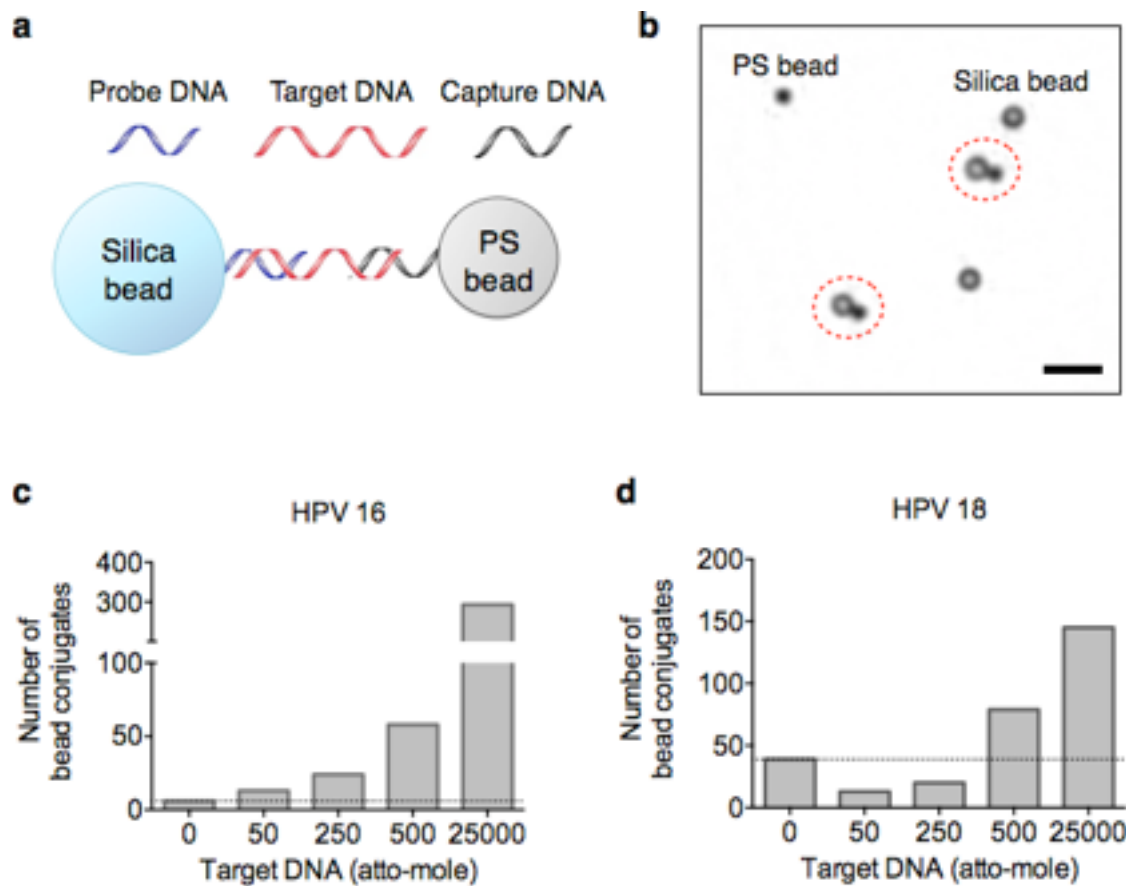
Fig. S16. HPV DNA detection using the D3 platform. (a) Two different types of microbeads were used to detect HPV DNA. Target DNA was captured by polystyrene (PS) beads conjugated with capture probes. Subsequently, silica beads with probe DNA were hybridized to form a bead dimer. **(b)** The D3 platform enumerate the number of PS-silica dimers to quantify the amount of target DNA. **(c, d)** Measurements with using serial dilutions of DNA target (without polymerase chain reaction amplification) showed the detection sensitivity in the atto-molar range for HPV
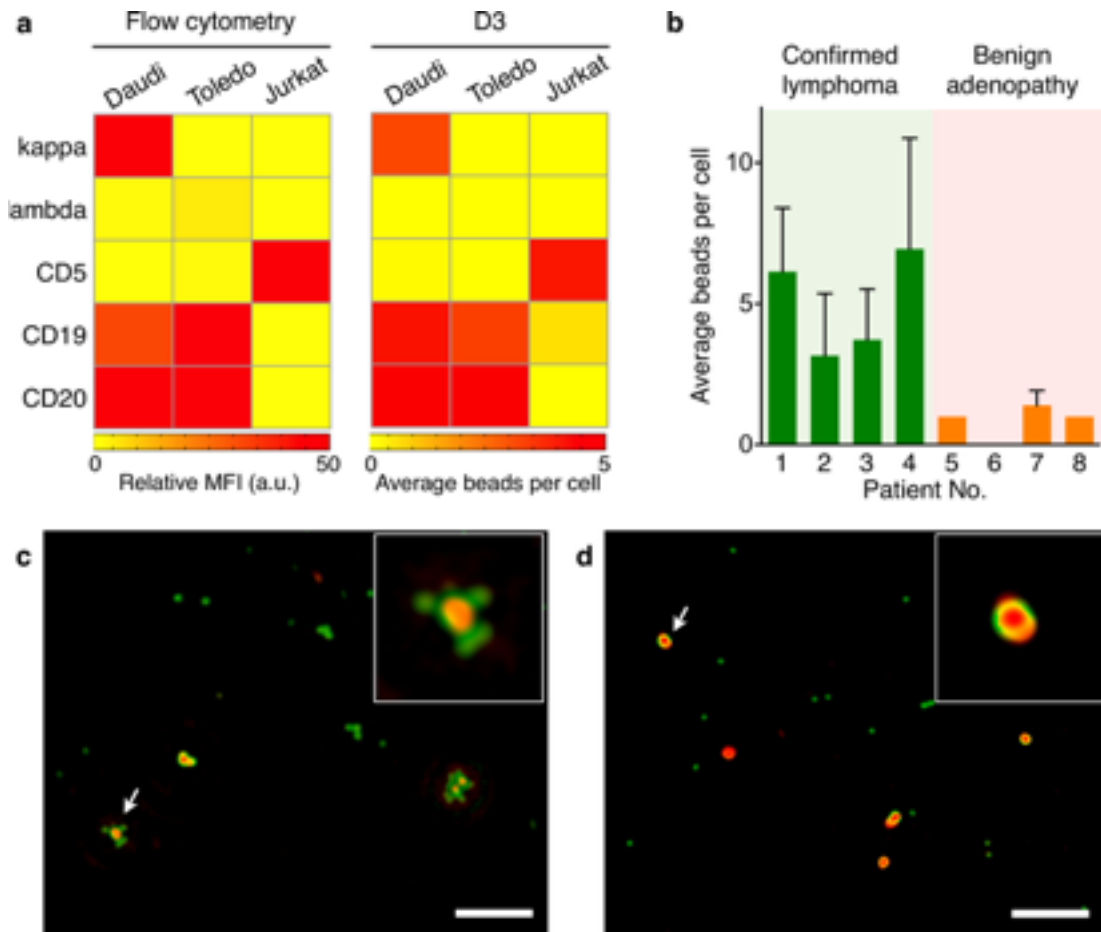
Fig. S17. Molecular profiling of clinical lymph node samples. (a) Expression levels of lymphoma-related diagnostic markers were profiled for a panel of lymphoma cell lines by flow cytometry and D3: Daudi (Burkitt's lymphoma); Toledo (diffuse large B-cell lymphoma); Jurkat (control T-cell leukemia). MFI, mean fluorescence intensity. a.u., arbitrary unit. **(b)** Based on the profiling data, we chose CD20 to analyze clinical samples. Fine needle aspirates of clinically suspicious lymph nodes from 8 patients were attained during clinically indicated biopsies. Samples were labeled with immunobeads specific to CD20. The average bead counts per labeled cell were significantly different between patients eventually diagnosed with lymphoma (n = 4) or benign (n = 4) disease (p = 0.005). Representative reconstructed image of cells from a lymphoma **(c)** and benign case **(d)** are shown. The insets are zoomed-in images of cells indicated by white arrows. Scale bar, 50 μm.

Supplementary References

1. Chung HJ, Castro CM, Im H, Lee H, Weissleder R (2013) A magneto-DNA nanoparticle system for rapid detection and phenotyping of bacteria. *Nat Nanotechnol* 8(5):369–375.